

# CURRENT LIMITATION BY HIGH TEMPERATURE SUPERCONDUCTORS AND BY CONDUCTING POLYMERS

M. Lindmayer, M. Schubert  
TU Braunschweig, Germany

## Abstract

The transition of materials from zero or low resistivity to comparatively high resistivity may be utilized for current limitation, enabling permanent fuses that don't have to be replaced after short circuit operation. This paper deals with two principles - superconductors and conducting polymers - and reports about experiments and simulations.

Mainly two ways are known to limit short circuit currents by using superconductors, the inductive and the resistive one. This paper concentrates on the resistive limiter. It directly uses the transition from superconductivity to normal conduction. Measurements of the resistivity of high temperature superconductors as a function of temperature and current density are presented. Based on these data, the performance of resistive limiters is simulated and the consequences are discussed.

Conducting polymers with a temperature-dependent transition from low to high resistivity are a similar way to limit short circuit currents. Based on measurements of the thermal and electrical properties of such polymers, the current-limiting behavior is simulated as well. The results are in good accordance with switching tests in a low voltage circuit.

## 1. Introduction

The principle of current limitation by elements that increase their resistance upon short-circuit has been known for a long time to the fuse community. In conventional fuses this is achieved by arcing after the element has fused. Circuit breakers use the establishment, prolongation and subdivision of an arc between quickly separating contacts. Another approach is the application of elements whose resistivity is either current- or temperature-dependent or both. In contrast to normal fuses they are reusable due to their reversible behavior. Such examples are

- permanent fuses with sodium as active metal, utilizing the reversible resistivity increase at melting and plasma formation [26],
- ceramic materials with positive temperature characteristics (PTC), such as barium titanate or vanadium oxide [27],
- superconductors, turning normal when their critical data, especially their critical current, is exceeded,
- temperature-dependent conducting polymers [28].

Of all these mechanism, the following presentation shall be concentrated on current limitation by superconductors and by temperature-dependent polymer materials, which have both been investigated by the authors recently. Their applications lie in different fields. While superconducting limiters are being developed mainly for medium voltage systems, the present use of polymer limiters lies in the low voltage field, ranging from the protection of electronic elements and circuits to motor protection.

## 2. Superconducting Current Limiters

Work on current limitation by means of superconductors has already been done before the discovery of high- $T_c$  superconductivity [2-7]. Because of the simpler cooling conditions - only liquid nitrogen is required instead of liquid helium - and several favorable physical properties, high temperature superconductors (HTSC) seem to own some advantages over low temperature superconductors for the use in current limiters [5], provided they will be available in shapes that can be handled technically. The further details in this chapter shall be concentrated to HTSC.

There are mainly two principles with many variants known, the inductive and the resistive limitation principle. It makes no sense to differentiate between them very strictly, because in both cases the change of superconductor resistance is generally utilized.

## 2.1 Inductive Limiters

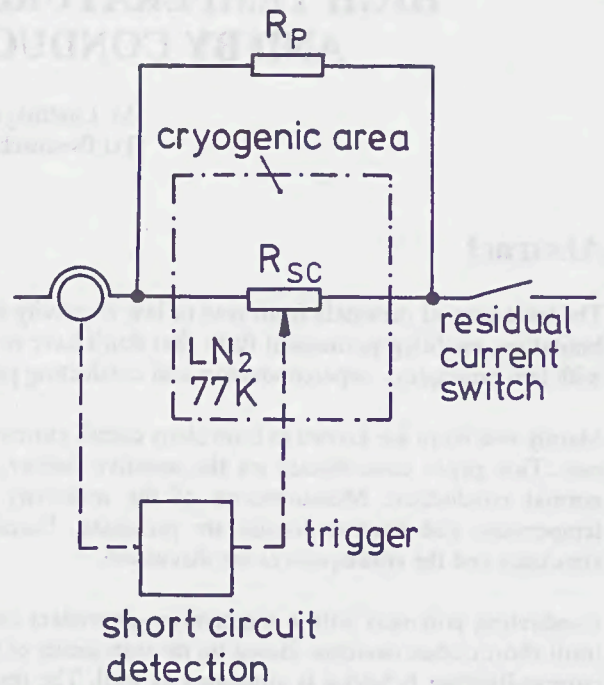
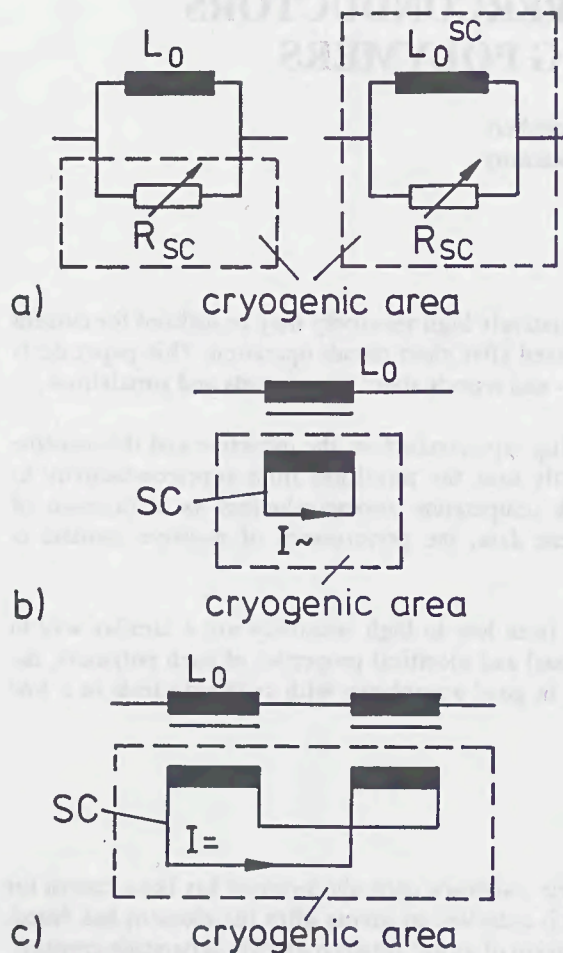


Fig. 2: Principle of resistive fault current limiter

Fig. 1: Inductive fault current limiters  
 a) inductance with resistive triggering  
 b) magnetic shielding, flux compensation  
 c) pre-magnetized saturation reactance

The group of inductive limiters [7,9,11,20] consists of a transformer or an inductance with at least one superconducting winding. Its impedance is changed upon the occurrence of a short-circuit. Some variants are summarized in fig. 1 [20]: Variant a) („inductance with resistive triggering“) consists of an inductance shunted by a superconductor. When its critical current is exceeded, the inductance becomes effective and limits the current. Fig. 1b („magnetic shielding“ or „flux compensation“) represents a transformer with a one-turn superconducting secondary winding. While under normal operation the impedance of the short-circuited transformer is low, the increased resistance of the secondary is transformed into the primary circuit when it becomes normal-conducting at overload. The type of fig. 1c is a series combination of two saturation reactances with superconducting DC pre-magnetization windings. Under normal conditions both cores remain saturated, resulting in low impedance. At overload, one of the cores, depending on the polarity, gets out of saturation and increases the resulting impedance. Many other variants have been suggested, e.g. superconducting three-phase differential transformers [11].

The advantage of inductive limiters is that most solutions do not need cryogenic bushings, and that they can be better realized by presently available HTSC materials. Their main drawback seems to be the considerable amount of iron needed. Due to the stray flux, the impedance ratio ON / OFF is limited.

## 2.2 Resistive Limiters

The other way is the resistive fault current limiter, fig. 2 [7,8,10,12,15]. It is arranged directly in series with each phase of the power circuit and consists of the cooled superconductor which limits the fault current by transition from the superconducting state to normal conduction, if necessary some linear or nonlinear resistive elements  $R_P$  in parallel, and a switch to finally interrupt the residual current. It may either be triggered by external pulses or utilize the natural quench when the critical current is exceeded. The further considerations are restricted to such resistive limiters.

## 2.2.1 Resistivity of HTSC Materials

To assess the realization of resistive HTSC fault current limiters, samples of different HTSC materials were measured with respect to their resistivity as a function of temperature, current, and magnetic field. Polycrystalline bulk material of  $Y_1Ba_2Cu_3O_x$  ("YBCO") and  $Bi_2Sr_2Ca_2Cu_3O_x$  ("BSCCO"), the latter manufactured by the "powder-in-tube" process [13,14] were investigated, as well as thin layers on ceramic substrates [19].

The sample length was several centimeters, the measuring length for voltage and resistivity between 5 and 10 mm. As an example typical for most materials, fig. 3 depicts the resistivity behavior of a BSCCO superconductor at nearly zero current and with different transport currents in a lin-log scale. The silver coating which would be prohibitive for current limitation was removed by an electrolytic process. The critical current of this sample at 77 K (temperature of liquid nitrogen) was  $\approx 1.8$  A (approx. 1500 A/cm<sup>2</sup>). Its  $T_C$  lies around 105 K. While the temperature is below the critical point  $T_C$ , the resistivity increases only weakly when the current is raised [16,17]. The curves meet all in one point (2) at a fraction of the full normal resistance, and continue independently of current beyond this point. To utilize the full span of resistivity, it is necessary to exceed the critical temperature.

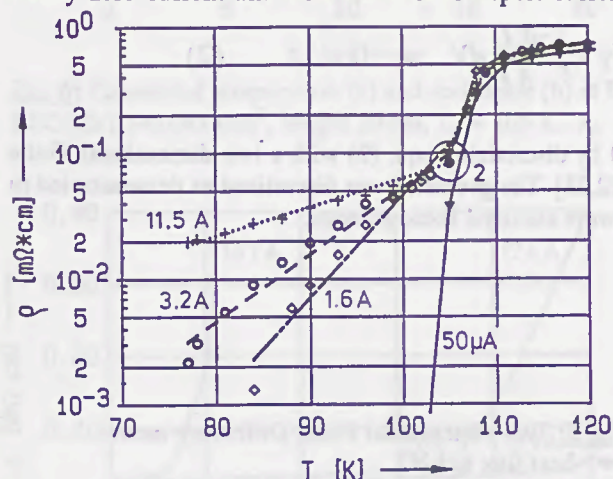


Fig. 3: Resistivity of BSCCO as a function of temperature and current.  $I_C \approx 1.8$  A at 77 K.

Fig. 3: Resistivity of BSCCO as a function of temperature and current.  $I_C \approx 1.8$  A at 77 K.

## 2.2.2 Simulation of HTSCs as Resistive Current Limiters

### 2.2.2.1 Method of Simulation

For simulations the dependence of the HTSC resistivity on current density and temperature must be modeled. Fig. 4 shows in a linear scale analytical approximations which were used for this purpose. They are described in detail in [19].

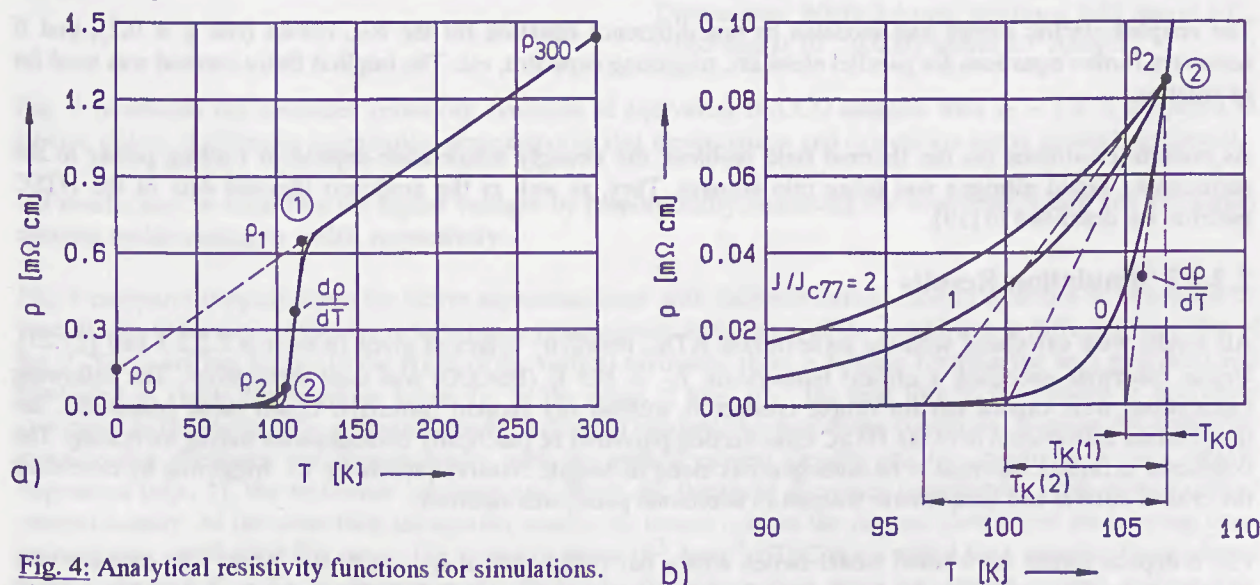


Fig. 4: Analytical resistivity functions for simulations. a) whole range b) magnification

The resistivity level, e.g.  $\rho_{300}$ , depends on the critical current density of the superconductor. The following dependence was taken from a summary of data [21]

$$\rho_{300} \cdot J_C^2 = 5.24 \cdot 10^{-3} \cdot J_C^{1.83}, \quad (1)$$

where  $\rho_{300} \cdot J_C^2$  in  $W/cm^3$  and  $J_C$  in  $A/cm^2$ .

This relation ( $\rho$  proportional to  $J_C^{-0.17}$ ) was used in the whole resistivity range to model fictive conductors with different critical current densities.

On the basis of these resistivity functions simulations of the electrical - thermal behavior of HTSC conductors as limiters together with the electric circuit were carried out.

The equation for the power balance per unit volume in integral form reads

$$\iiint \frac{J^2}{\sigma} dV + \iiint \text{div}(\lambda \text{ grad } T) dV - \iiint \gamma c_p \frac{\partial T}{\partial t} dV = 0 \quad (2)$$

The HTSC or HTSC/substrate combinations were modeled by discretizing equ. (2) with a two-dimensional Finite Difference Method (FDM). More details are described in [22,23]. The geometry was discretized as demonstrated in fig. 5. The properties across the third dimension (width  $w$ ) were assumed homogeneous.

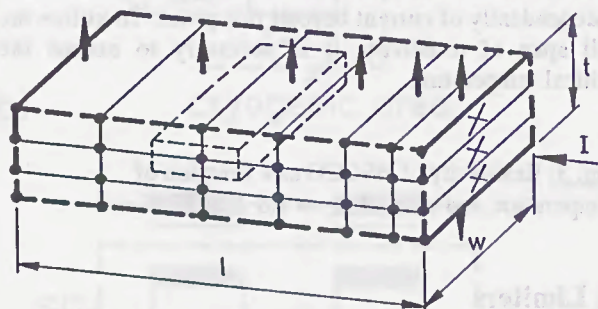


Fig. 5: Two-dimensional Finite Difference model  
 → heat flux to LN2  
 X current flow, perpendicular  
 • grid points

The solution of the thermal balance was coupled at each time step to the current flow field. The current distribution in the conductor was assumed to follow the local resistivity which in turn depends on the local current density and temperature. This required the application of iterations. The unknown current distribution was gained by solving the second order partial differential equation of the current flow field by a Finite Difference scheme similar to that of the thermal balance.

The coupled electric circuit was modeled by one difference equation for the R-L circuit ( $\cos \varphi = 0.2$ ), and if necessary further equations for parallel elements, triggering capacitor, etc. The implicit Euler method was used for its solution.

As random conditions for the thermal field problem, the strongly temperature-dependent cooling power to the surrounding liquid nitrogen was taken into account. They, as well as the nonlinear thermal data of the HTSC material are described in [19].

### 2.2.2.2 Simulation Results

All results were calculated with the standardized HTSC resistivity values as given in section 2.2.2.1 and [22,23]. Unless otherwise specified, a critical temperature  $T_C \approx 105$  K (BSCCO) was used throughout. The following calculations were carried out for simple conductors without any support materials. Under these conditions, the temperature distribution over the HTSC cross section proved to be practically homogeneous during switching. The conductor is further assumed to be homogeneous along its length. Natural quenching, i.e. triggering by exceeding the critical current and temperature without an additional pulse, was assumed.

Fig. 6 depicts results for a small model switch with a flat HTSC tape of  $J_C = 1.5 \cdot 10^3$   $A/cm^2$ . Its data are very close to the measurements of fig 3. Up to a threshold of 13 A or  $7 \cdot J_C$  the HTSC is not fully driven into normal conduction, i.e. the critical temperature is not exceeded. The heat is completely dissipated to the LN2 coolant at a stable temperature well below  $T_C$ . A slightly higher current leads to power losses that exceed the maximum of 0.12 Watts per square millimeter of the conductor surface that can be dissipated into the nitrogen bath. The conductor heats up and finally quenches after 14 ms. The tripping time  $t_T$  is defined as the time when 110 K are reached.

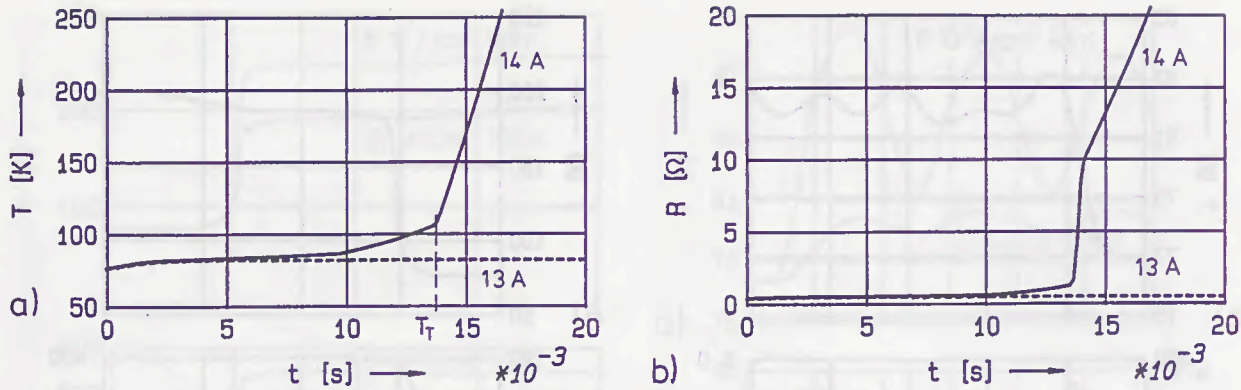


Fig. 6: Calculated temperature (a) and resistance (b) at DC load. BSCCO  $1.5 \cdot 0.085 \text{ mm}^2$ , length 20 cm,  $T_C = 105 \text{ K}$ ,  $J_C = 1.5 \cdot 10^3 \text{ A/cm}^2$ .

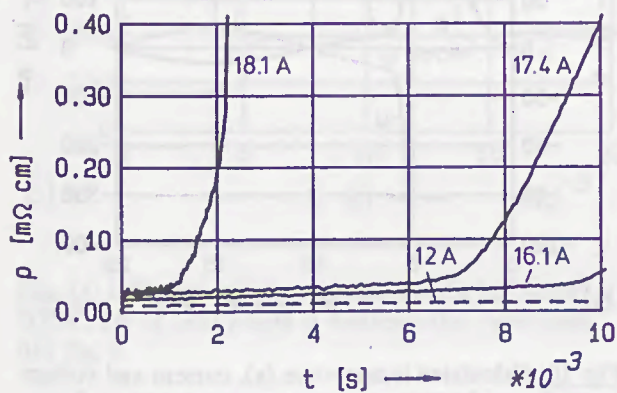


Fig. 7: Measured resistivity vs. time of BSCCO sample with  $I_C \approx 1.8 \text{ A}$ .

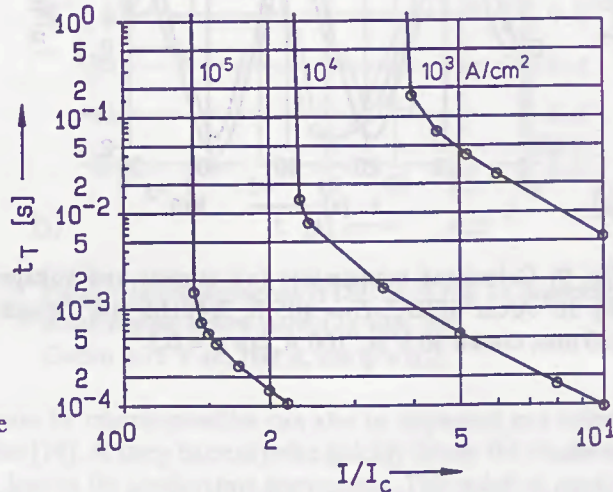


Fig. 8: Calculated tripping time vs. normalized current for HTSCs with different critical current densities. Dimensions: Width 3.4 mm; thickness 0.85 mm at  $10^3$ , 0.085 mm at  $10^4$ , 0.0085 mm at  $10^5 \text{ A/cm}^2$ .

Fig. 7 represents the measured resistivity evolution of equivalent BSCCO samples with  $I_C \approx 1.8 \text{ A}$  subjected to current pulses of different magnitudes, demonstrating that measurement and calculation are in general agreement.

All results may be scaled up for higher voltages by proportionally increasing the conductor length and for higher currents by increasing its width, respectively.

Fig. 8 compares tripping times for fictive superconductors with different critical current densities at impressed dc load. It should be noticed that the ratio between cross-section and surface of the conductors is different from that of fig. 7. There are two limits: In the range of the vertical asymptote there is balance between the heat generated and dissipated at stable temperatures below  $T_C$ . In the range at high  $I/I_C$  the heat flux to the coolant is negligible compared to the electrically generated power, leading to adiabatic heating of the conductor. Because the conductor cross-section decreases anti-proportionally with the critical current density and the resistivity is only weakly dependent (equ. 1), the resistance increases and hence the threshold decreases considerably with higher critical current density. At the same time the smaller mass to be heated reduces the thermal inertia and the tripping time, respectively, in the adiabatic range. Fig. 8 reveals that a  $10^3 \text{ A/cm}^2$  HTSC is not suited for a resistive limiter based upon exceeding  $T_C$ . To limit ac currents effectively, the release time must not exceed several milliseconds. Conductors of at least  $10^4 \text{ A/cm}^2$  critical current density are necessary.

Figs. 9 and 10 represent the temperature, voltage and current evolution of small model switches under ac short circuit conditions. In both cases the critical current lies at 28.9 A. To stay well below the critical current under normal operating conditions, the rated RMS current of such a limiter would lie around 10 A. In these and all other ac calculations the moment of circuit closure lies at voltage zero, causing maximum dc component. Fig. 9 underlines the fact already known from fig. 8. The threshold of the  $10^3 \text{ A/cm}^2$  conductor and its thermal inertia

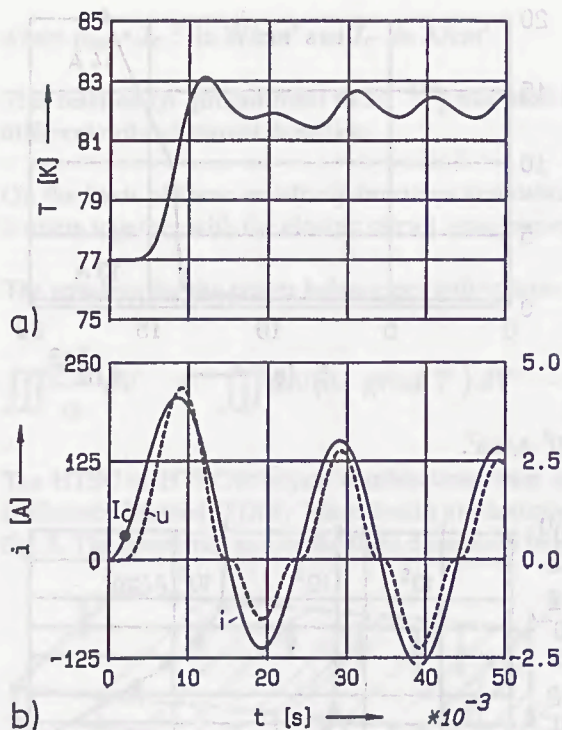


Fig. 9: Calculated temperature (a), current and voltage (b):  $10^3$  A/cm<sup>2</sup> HTSC,  $T_C = 105$  K,  $3.4 \cdot 0.85$  mm<sup>2</sup>, length 200 mm, circuit 30 V ac, 100 A,  $\cos \varphi = 0.2$ .

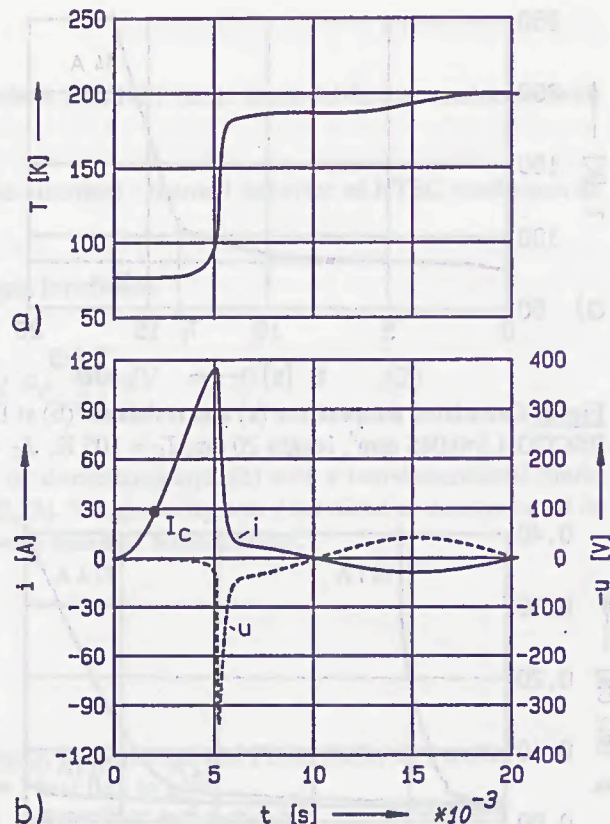


Fig. 10: Calculated temperature (a), current and voltage (b).  $10^4$  A/cm<sup>2</sup> HTSC,  $T_C = 105$  K,  $3.4 \cdot 0.085$  mm<sup>2</sup>; other conditions like fig. 9.

prevent any current limitation. The situation becomes different with a  $10^4$  A/cm<sup>2</sup> conductor (fig. 10). About 3 ms after the critical current is exceeded, the critical temperature is reached, the transition to the state of normal conduction quickly takes place, and the current is limited before its prospective maximum. The temperature rises steeply. From coarse energy considerations, the quantity of heat additionally stored in the conductor during this time is the sum of the energy  $1/2 L i^2$  stored in the circuit inductance immediately before and the energy supplied from the circuit during the transition. The following residual current is determined by the normal resistance; as it would cause further temperature increase, it has to be interrupted after a few ten milliseconds by an additional load switch in series. The voltage across the conductor shows a strong peak during the fast transition. It may be unacceptably high unless reduced by parallel elements.

Technically manufactured superconductors would be subject to certain inhomogeneities, i.e. statistical fluctuations of critical current density and critical temperature along the conductor. This influence was also studied. Fig. 11 presents the temporal temperature evolution of the same  $10^4$  A/cm<sup>2</sup> limiter as before. It was assumed that one per cent of the total HTSC length is weaker, with both lower  $J_C$  and  $T_C$ . Current and voltage do not differ substantially from those of fig. 10. The weaker part turns normal first and quickly overheats. The higher the grade of inhomogeneity, the more uneven is the temperature distribution. This problem increases as the critical current density and hence the conductor mass decrease. The longitudinal quench propagation by thermal conduction within the ceramic superconductor is by far too slow to equalize this behavior.

There are several methods conceivable to overcome the inhomogeneity problem:

It could be an alternative not to exceed the critical temperature but to operate in the area below  $T_C$  and above  $J_C$  in the "foot region" left of point (2), figs. 3, 4. As the resistivity is much smaller, the conductor length would have to be increased considerably, by more than one order of magnitude. Ac losses [25] would increase by the same ratio. Fig. 12 shows simulation results for the same conductor as in fig. 11, however with only 1/40 of the system voltage per unit length. For the same voltage the length would have to be increased by 40. The two critical currents are marked by points on the current curve. The results show that there is an effective current limitation and that the temperatures stay well below the critical points of 95 and 105 K, respectively.

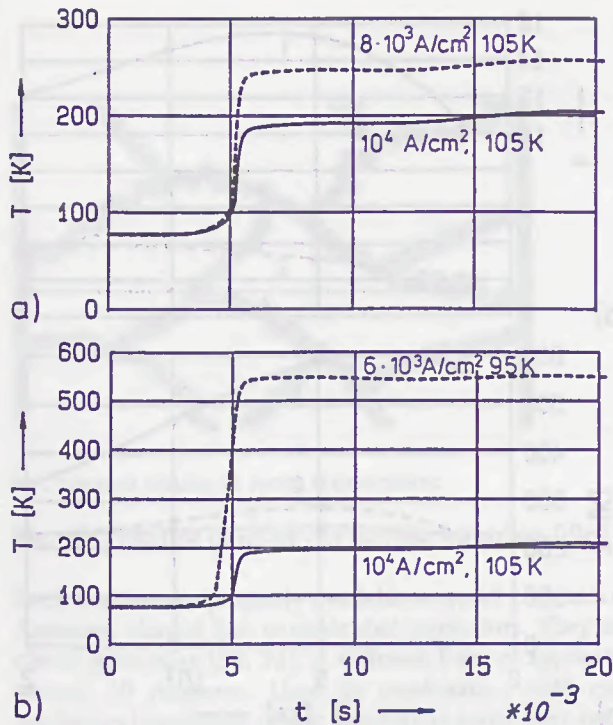


Fig. 11: Influence of inhomogeneities of a  $10^4$  A/cm<sup>2</sup> HTSC. 1% of total length is weaker; other conditions like fig. 9.

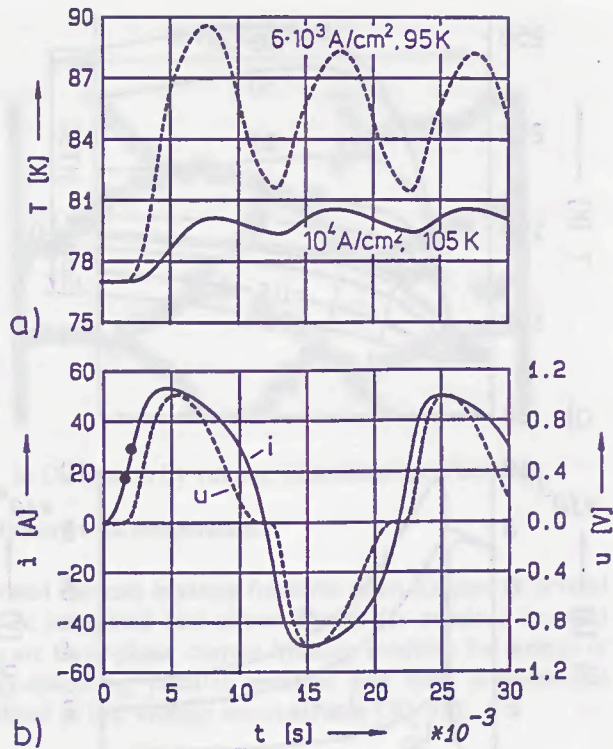


Fig. 12: Inhomogeneous HTSC as in fig. 11, working in the regime below point (2), figs. 3-5. Circuit 0.75 V ac, 100 A,  $\cos \varphi = 0.2$ .

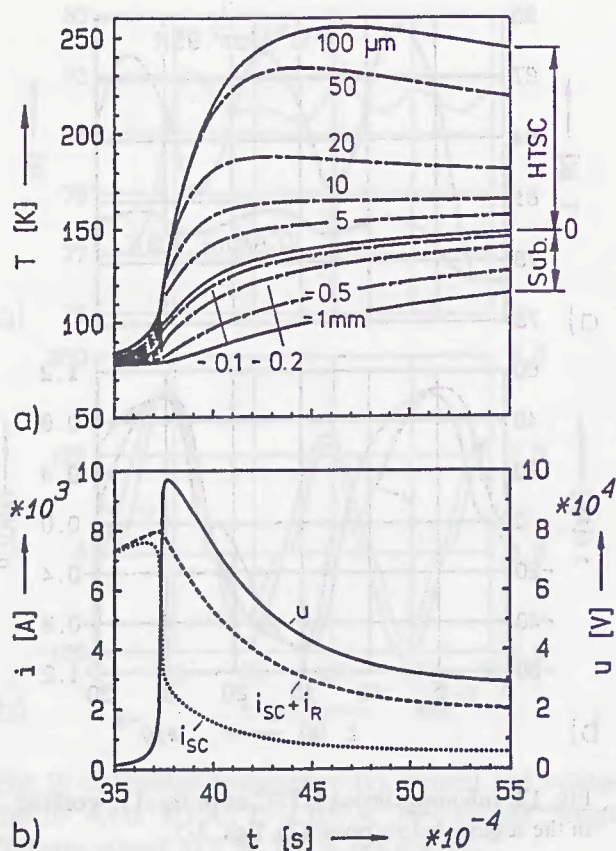
As further simulations show, the problem of uneven release by inhomogeneities can also be improved to a certain degree by appropriate triggering from a charged capacitor [19]. A steep current pulse quickly drives the conductor into normal conduction - again by heating over  $T_c$  - and lessens the temperature unevenness. This solution needs a rather high trigger energy and is costly and space-consuming.

Triggering by a magnetic field could be another alternative. The effect is similar to exceeding the critical current, i.e. only a fraction of the full resistivity span is available at the first moment, and the conductor subsequently has to heat up above the critical temperature. In any case, the conductor has to be placed in a rather even magnetic trigger field to avoid additional inhomogeneities.

Thermal and electrical stabilization by close contact with well-conducting metal is a proved means to equalize the effect of local inhomogeneities. It has been used in low temperature superconductor technology for some time, where metallic niobium-based superconductors are stabilized by copper or CuNi alloy [2,10]. While for most applications, like cables or machine windings, the stabilizing material should have as low electrical and thermal resistance as possible, a resistive HTSC limiter would need a stabilizer with high electrical resistance [10]. Provided the technological problems can be solved, a sandwich tape consisting of resistive material as a support for a layer of HTSC could be the solution.

Fig. 10 has already demonstrated that the fast resistance transition is accompanied by a sharp voltage peak several times as high as the peak system voltage. For even higher  $J_c$  such as  $10^5$  A/cm<sup>2</sup> the transition occurs still faster and hence the overvoltage is still higher. At the same time the temperature rise increases because the available conductor mass is reduced. Additional elements parallel to the superconductor (resistor or voltage limiter) are a means to reduce both the voltage and temperature stress.

Because the ceramic HTSC materials are rather brittle, they need a mechanical support anyhow. This could be a ceramic substrate. Its heat conduction and heat capacity would additionally contribute to consume the energy produced at switching. Some simulation results with such an arrangement are discussed subsequently. It consists of a fictive 50 m long, 0.1 mm thick and 50 mm wide homogeneous HTSC layer on a ceramic substrate of 1 mm thickness (aluminum oxide, thermal data from [24]). The critical current is 5000 A, yielding a nominal current around 2000 A. The conditions are equivalent to one phase of a medium voltage power distribution system.



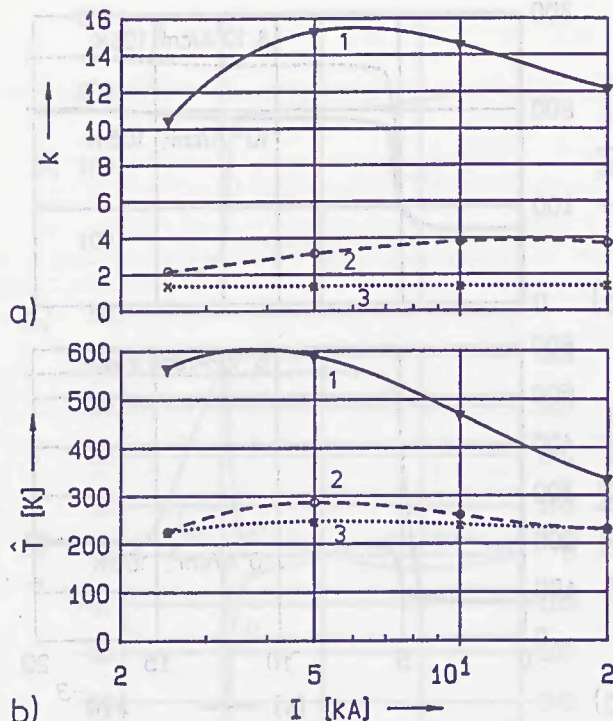
**Fig. 13:** Calculated temperatures (a), currents and voltage (b) for a fictive 50 m long sandwich of  $10^5$  A/cm<sup>2</sup>, 105 K HTSC,  $50 \cdot 0.1$  mm<sup>2</sup> on 1mm Al<sub>2</sub>O<sub>3</sub> substrate. Circuit 20 kV ac, 10 kA,  $\cos \varphi = 0.2$ , external resistor 20  $\Omega$  parallel to the HTSC; numbers are coordinates of the (uneven) grid across the conductor / substrate thickness;  $i_{sc} + i_R$  total current,  $i_{sc}$  current in superconductor

Fig. 13 shows exemplary courses of voltage, superconductor current, and current in a parallel resistor during a narrow time span around the transition. The temperature distribution across the sandwich thickness reveals that within the conducting layer where the heat is generated there is a strong negative temperature gradient towards the still cool substrate, causing strong heat flux towards it. It should be noticed that the grid spacing is not equidistant!

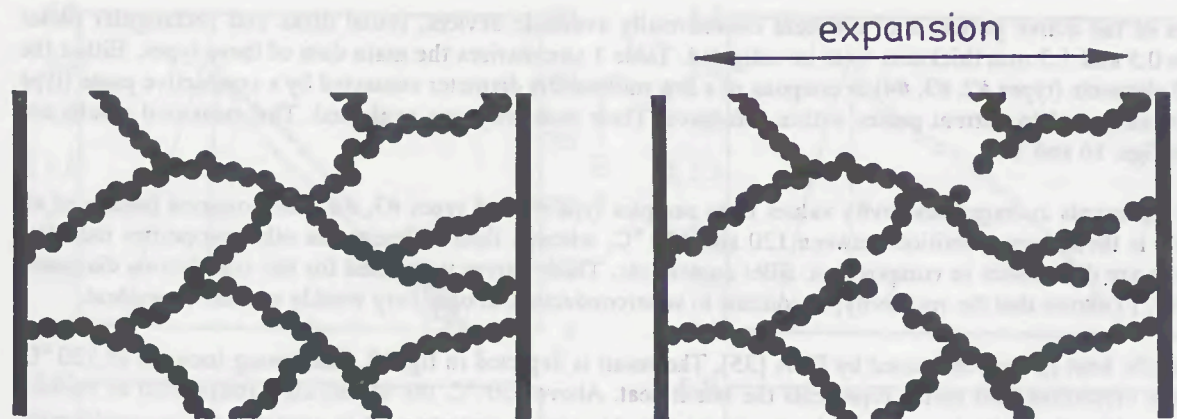
Fig. 14 summarizes computed results of the overvoltage factor (peak voltage related to the peak RMS voltage) and the maximum temperature at the hottest location as a function of the short circuit current for the above arrangement without parallel elements, and with a parallel 20  $\Omega$  resistor and an ideal 40 kV voltage limiter, respectively. While the application of a  $10^5$  A/cm<sup>2</sup> HTSC without any parallel path would be prohibitive for both voltage and temperature reasons, the situation strongly improves by adequately chosen parallel elements. Fig. 13 demonstrates that a considerable part of the total current flows through the bypass when the superconductor has started to go normal, thus preventing excess heating and too fast resistance rise accompanied by overvoltages.

### 3. Current Limitation by Conducting Polymers with PTC Characteristics

Materials with strongly increasing resistivity above a certain threshold temperature, though different in the physical nature, show many similarities with superconductors when their critical temperature is reached. BaTiO<sub>3</sub> and V<sub>2</sub>O<sub>3</sub> ceramics with such positive temperature coefficients have been known for some time [29]. In the last years, conducting polymers have gained industrial application. They generally consist of polymers like polyethylene filled with conducting particles, especially carbon black [28, 30, 31, 32, 34]. As shown in fig. 15, the filler particles form bridges of low resistivity when in the state of nominal load. When the crystalline melting point is exceeded at about 125 °C, the polymer matrix expands, the bridges are ruptured, and the resistivity is increased by orders of magnitude. This process is reversible and enables the design of current-limiting devices which act as permanent fuses.



**Fig. 14:** Overvoltage factor  $k$  (a) and temperature at the hottest point (b) for the fictive HTSC/substrate combination as in fig. 13. 1 without parallel element, 2 resistor 20  $\Omega$ , 3 voltage limiter 40 kV.



a) Coherent chains at room temperature

b) Disruption by volume expansion upon heating

Fig. 15: Principle of resistivity increase of carbon-filled polymers with temperature.

Such limiters are presently available as small elements of rated currents between fractions of an Ampere to several Amperes, shaped like ceramic disk capacitors. They may be integrated into circuit boards for overload or short circuit protection [32, 33]. A different form of application are three-phase current-limiting modules for ratings of several 10 Amperes. Used in combination with energy-absorbing parallel resistors and with conventional mechanical miniature circuit breakers in series they are utilized as low voltage motor starters [30, 31].

In order to study the mechanisms of these conducting polymers in detail, their electrical as well as their thermal properties were measured. Based on these data, simulations of the coupled thermal and electrical process similar to those described in the preceding chapter were carried out and compared with measurements.

### 3.1 Electrical and Thermal Properties of PTC Polymers

Type	Rated Current A	Rated Voltage V	Dimensions of Polymer Disk mm	Rated Current Density A/cm <sup>2</sup>	Density of Polymer g/cm <sup>3</sup>	Resistivity at 25 °C Ω cm	References
#1	36	400, 3~	60 • 35 • 1.3	1.71	1.0	2	[30, 31]
#2	3.75	50 AC/DC	∅ 19 • 0.55	0.75	1.46	3,5	[28, 32]
#3	0.5	60 AC/DC	∅ 6.4 • 0.5	1.55	1.33	5	[28, 32]
#4	0.25	60 AC/DC	∅ 4.3 • 0.5	1.72	1.02	5.5	[28, 32]

Table 1: Characteristics of the investigated current limiters with conducting polymers

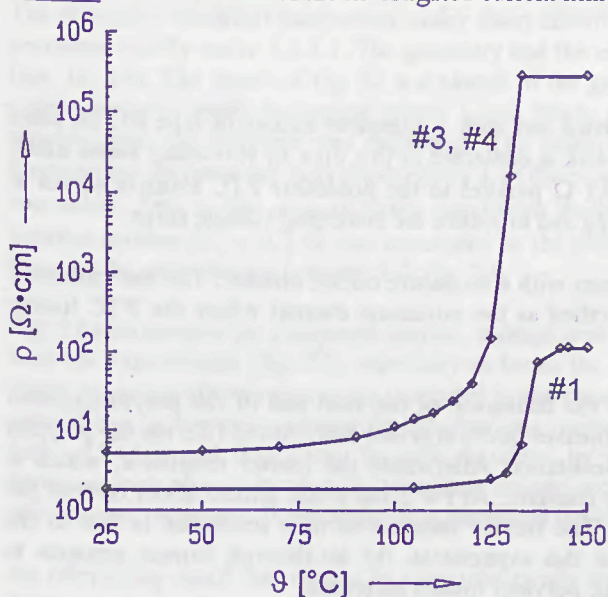


Fig. 16: Typical curves of resistivity vs. temperature for different types of conducting polymers.

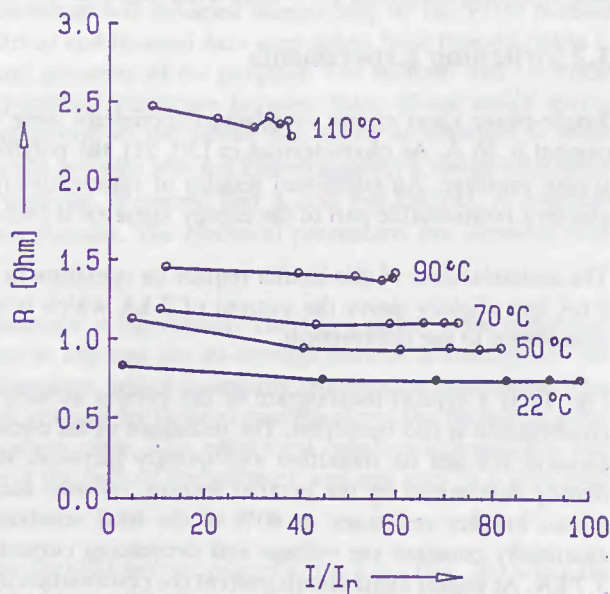
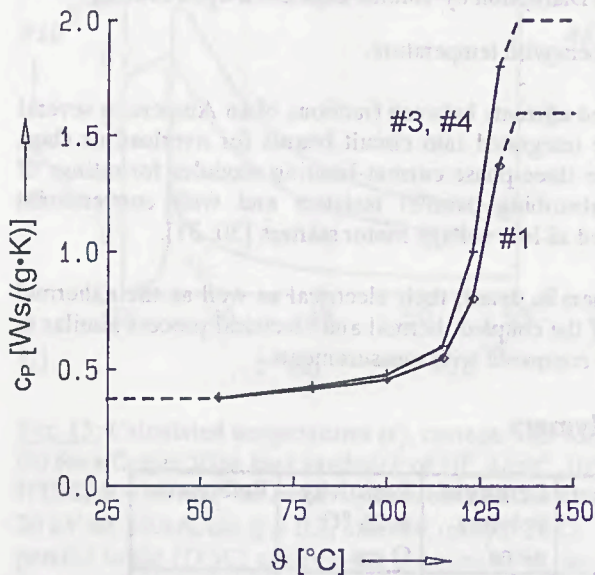


Fig. 17: Resistivity at different temperatures as a function of normalized current. Type #3.

Samples of the active polymers of different commercially available devices, round disks and rectangular plates between 0.5 and 1.3 mm thickness were investigated. Table 1 summarizes the main data of these types. Either the original elements (types #2, #3, #4) or coupons of a few millimeters diameter contacted by a conductive paste (type #1) were subjected to current pulses within a furnace. Their resistivity was evaluated. The measured results are given in figs. 16 and 17.

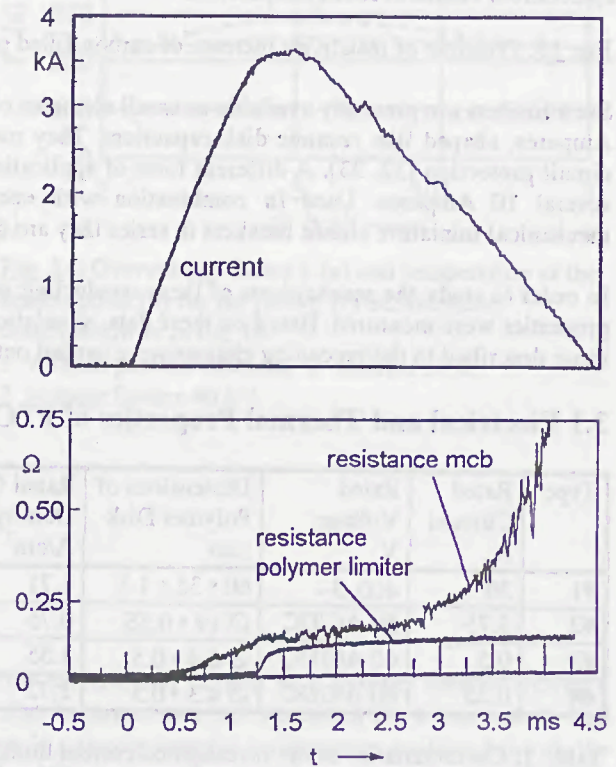
Fig. 16 represents averaged resistivity values from samples type #1 and types #3, #4. The common feature of all materials is their steep transition between 120 and 130 °C, whereas their difference in other properties indicates that there are differences in composition, filler content etc. These curves were used for the simulations discussed later. Fig. 17 shows that the resistivity, in contrast to superconductors, is only very weakly current-dependent.

The specific heat  $c_p$  was measured by DTA [35]. The result is depicted in fig. 18. The strong increase at 120 °C, where the crystalline part melts, represents the latent heat. Above 130 °C, the values are extrapolated as dashed. The thermal conductivity  $\lambda$  could not be measured yet. At room temperature, it is expected to lie considerably above that of pure polyethylene.



↑ Fig. 18: Specific heat of conducting polymers  
 ---- extrapolated

Fig. 19: Switching test of type #1 with parallel resistor →  
 $\approx 0.1 \Omega$  and miniature circuit breaker (mcb) in series.  
 250 V, 50 Hz, 8 kA,  $\cos \varphi = 0.6$ , making angle 53°.



### 3.2 Switching Experiments

Single-phase short circuit switching experiments were carried out with a complete limiter of type #1. Its rated current is 36 A. As characterized in [30, 31], the polymer disk is contacted in this area by two metal plates under spring pressure. An additional resistor of approximately 0.1  $\Omega$  parallel to the nonlinear PTC element serves to absorb a considerable part of the energy liberated at switching and to reduce the switching voltage surge.

The technical data of this limiter require its operation in series with a miniature circuit breaker. The test current of 8 kA lies slightly above the current of 7 kA which is specified as the minimum current where the PTC limiter contributes to the interruption.

Fig. 19 is a typical oscillogram of the current as well as the resistance of the mcb and of the polymer/resistor combination at this operation. The resistance of the circuit breaker (mcb) is raised first. At  $t = 1.25$  ms the polymer element reaches its transition and quickly increases its resistance. Afterwards the limiter resistance, which is mainly determined by the parallel resistor, remains nearly constant. At  $t = 2$  ms it has gained about 60% of the circuit breaker resistance or 40% of the total resistance. The further increase of mcb resistance is due to the essentially constant arc voltage and decreasing current. In this experiment, the let-through current amounts to 3.7 kA. At higher short circuit current the contribution of the polymer limiter increases.

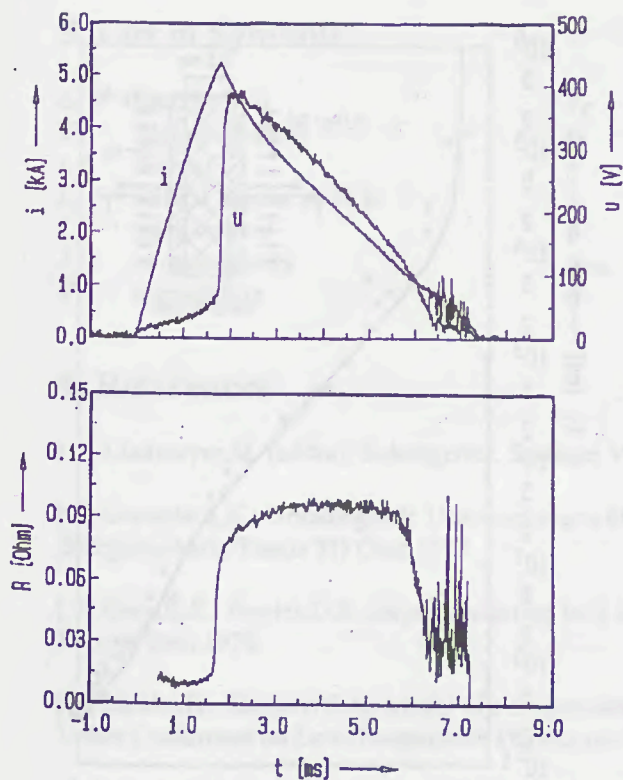


Fig 20: Switching test of type #1 with parallel resistor  $\approx 0.1 \Omega$ , without additional mcb. Circuit conditions as in fig. 19.

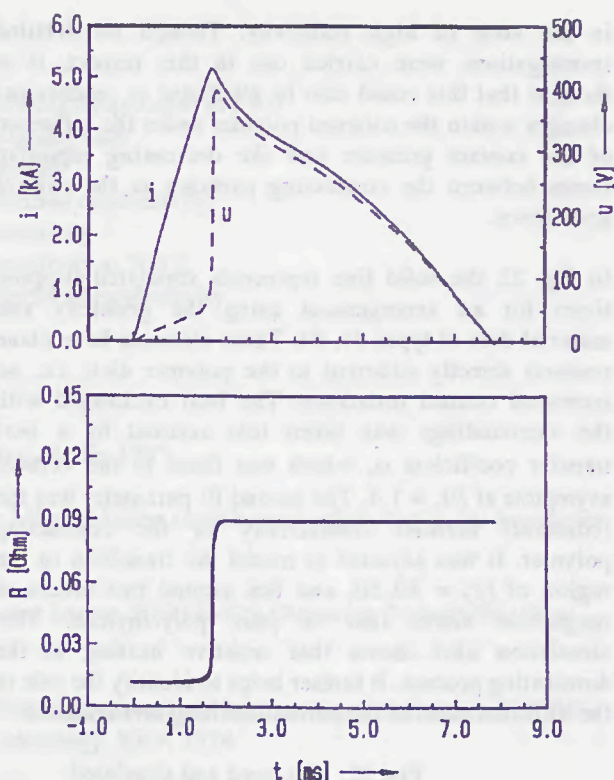


Fig 21: Simulated current limitation by type #1 with parallel resistor  $0.1 \Omega$ , without mcb. Circuit conditions as in fig. 19.

Fig. 20 represents an experiment under the same conditions, where, beyond the specifications, no additional circuit breaker was used. Instead, a thyristor in the test circuit limited the current flow to one half cycle. This time the current is effectively limited to  $\approx 5$  kA by the polymer / resistor combination. The sudden resistivity decrease at  $t \approx 6$  ms will be discussed later, as well as the simulation results of fig. 21.

In fig. 22 the tripping time at DC load vs. the normalized current, measured with limiter elements of types #3, #4 (table 1) is plotted and also compared with results of computations. It will be discussed later.

### 3.3 Simulation of Short Circuit Limitation and Comparison with Measurements

The thermal - electrical interaction under short circuit conditions was modeled numerically by the FDM method described briefly under 2.2.2.1. The geometry and the electrical and thermal data were taken from type #1 (table 1, figs. 16, 18). The insert of fig. 22 is a sketch of the general geometry of the polymer. The thermal and electrical connection was made by copper plates 1 mm thick. Any contact resistance between these plates under spring pressure and the polymer was neglected. The outer temperature of the plates was taken as constant = room temperature. Because the heat conductivity  $\lambda$  of the conducting polymer was not known exactly, a rough estimation was taken. Due to the near-adiabatic conditions during tripping, it proved that  $\lambda$  was not critical. A constant parallel resistor  $R_p = 0.1 \Omega$  was connected to the polymer element. The electrical parameters are identical with those of the experiments (chapter 3.2, fig. 20).

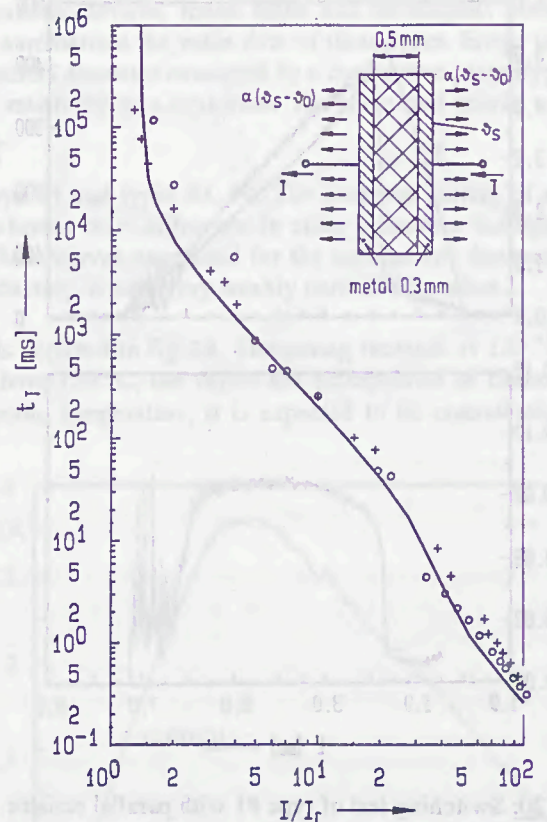
Fig. 21 summarizes the computed current, voltage, and resistance of the limiter. There is a rather good agreement with the experiments (fig. 20), especially as far as the time to trip and the let-through current is concerned. The slight deviation afterwards can be attributed to the parallel resistor, which is actually temperature-dependent. This coincidence is a strong evidence that the limiting process is initiated by thermal heating above the transition point  $120 - 130^\circ\text{C}$ , and that it can be well described by the above data. The agreement between computation and measurements also yields that the transition mainly occurs in the bulk of the polymer, and not only in a thin layer of increased resistance at the contacts as supposed in [30].

An interesting detail that cannot be explained purely by this thermal process occurs at  $t = 6$  ms (fig. 20) when the decreasing current gets below 1.5 kA. The resistance quickly drops, while the simulation yields much higher times to cool down. In [30] the fast recovery is explained by the fact that only a thin layer at the contact plates has been

in the state of high resistivity. Though no detailed investigations were carried out in this respect, it is thought that this could also be attributed to mechanical changes within the softened polymer under the influence of the contact pressure and the decreasing repulsive forces between the conducting particles as the current goes down.

In fig. 22 the solid line represents simulated tripping times for an arrangement using the geometry and material data of types #3, #4. These elements have plane contacts directly adherent to the polymer disk, i.e. no increased contact resistance. The heat exchanged with the surroundings was taken into account by a heat transfer coefficient  $\alpha$ , which was fitted to the vertical asymptote at  $I/I_r \approx 1.4$ . The second fit parameter was the (constant) thermal conductivity of the conducting polymer. It was adjusted to model the transition in the region of  $I/I_r = 30..50$ , and lies around two orders of magnitude above that of pure polyethylene. This simulation also shows that resistive heating is the dominating process. It further helps to identify the role of the different parts of the current-limiting arrangement.

Fig. 22: Measured and simulated tripping characteristics.  
+ type #3; o type #4



#### 4. Summary and Conclusion

The transition behavior between superconducting and normal-conducting state of high temperature superconductor materials was investigated experimentally with respect to the application in resistive fault current limiters. When the critical current is exceeded, a relatively weak resistivity increase occurs first. To utilize the full resistivity stroke, the critical temperature must be exceeded. By using the measured dependencies, simulations of the problem of two-dimensional dynamic thermal field in the superconductor together with the electric circuit were carried out. When the limitation is based on exceeding  $T_c$ , the critical current density  $J_c$  of the HTSC must be at least  $10^4$  A/cm<sup>2</sup>. Inhomogeneities in  $T_c$  and  $J_c$  along the conductor may cause problems with uneven transition to normal conductance. Some possibilities to overcome this problem are discussed. Especially with high  $J_c$  conductors considerable overvoltages may result at switching. They as well as excess heating of the conductor may be reduced by parallel elements.

While the general function of current limiters with HTSCs is well understood, the main problem presently lies in the development of the material. It should have high current density, good homogeneity and low ac losses, it should be available in long lengths, and should be well deformable. Intensive research work is going on in this field worldwide.

For low voltage circuit breakers the expenditure would be much too high for superconductors that have to be cooled in an LN<sub>2</sub> bath - and there are no room temperature superconductors in sight yet. The use of nonlinear temperature-dependent conducting polymers for current limitation could be a promising supplement or replacement for mechanical low voltage breakers. Similar to the work on HTSCs, electrical and thermal data of different carbon-filled disc- or plate-shaped polymer elements were measured. They were also used in simulations of the thermal - electrical behavior of such polymer plates as current limiters. For comparison, short circuit switching tests were carried out. The coincidence between the measurements and simulations shows that resistive heating above the crystalline melting point ( $\approx 125$  °C) is the effect responsible for the limitation, and that their tripping can be well modeled. The sudden resistance drop on decreasing current slope would need further investigations for a satisfactory explanation..

## 5. List of Symbols

$c_p$	specific heat	$T_c$	critical temperature at $I = 0$
$dV$	volume element	$t_T$	tripping time
$i, I$	current	$\gamma$	density
$I_c$	critical current at 77 K	$\lambda$	thermal conductivity
$I_r$	rated current	$\rho$	resistivity
$J$	current density	$\rho_{300}$	resistivity at 300 K
$T$	temperature	$\sigma$	electrical conductivity

## 6. References

- [ 1] Lindmayer, M. (editor): Schaltgeräte. Springer Verlag, Berlin 1987.
- [ 2] Grawatsch, K.: Grundlegende Untersuchungen über Möglichkeiten supraleitender Schalter in der kryogenen Energietechnik. Thesis TH Graz 1973.
- [ 3] Gray, K.E., Fowler, D.E.: Superconducting fault current limiter. EPRI E-329 (Research Project 328, Final Report) Dec. 1976.
- [ 4] Menke, H., Shishov, Y.A.: Model of a superconducting high current and high voltage interrupter. 18th All-Union Conference on Low-Temperature Physics and Technology, Kiev, 1974.
- [ 5] Bogner, G.: Kabel, Schalter und Transformatoren. VDI-Bericht 733 (1989) pp. 153-166.
- [ 6] Weber, R.: Supraleiter sichert hohe Spannungen. VDI-Nachrichten No. 06-24-1992 pp. 34-35.
- [ 7] Giese, R.F., Runde, M.: Fault current limiters. Argonne National Laboratory, Nov. 1991.
- [ 8] Ikegami, T., Yamagata, Y., Ebihara, K., Nakajima, H.: Application of high  $T_c$  superconductor to current limiting devices. IEEE Trans. on Applied Superconductivity 3 (1993) pp. 566-569.
- [ 9] Fleishman, L.S., Bashkirov, Y.A., Aresranu, V.A., Brissette, Y., Cave, J.R.: Design considerations for an inductive high  $T_c$  superconducting fault current limiter. IEEE Trans. on Applied Superconductivity 3 (1993) pp. 570-573.
- [ 10] Verhaege, T., Tavergnier, J.P., Agnoux, C., Cotteville, C., Laumond, Y., Bekhaled, M., Bonnet, P., Collet, M., Pham, V.D.: Experimental 7.2 kV<sub>rms</sub>/1 kA<sub>rms</sub>/3 kA<sub>peak</sub> current limiter system. IEEE Trans. on Applied Superconductivity 3 (1993) pp. 574-577.
- [ 11] Shimizu, S., Tsukamoto, O., Ishigohka, T., Uriu, Y., Ninomiya, A.: Equivalent circuit and leakage reactances of superconducting 3-phase fault current limiter. IEEE Trans. on Applied Superconductivity 3 (1993) pp. 578-581.
- [ 12] Lindmayer, M., Schubert, M.: Resistive fault current limiters with HTSC - measurements and simulation. IEEE Trans. on Applied Superconductivity 3 (1993) pp. 884-888.
- [ 13] Tenbrink, J., Wilhelm, Heine, K., Krauth, H.: Development of technical high- $T_c$  superconductor wires and tapes. IEEE Trans. on Applied Superconductivity 3 (1993) pp. 1123-1126.
- [ 14] Haldar, P. et. al.: Fabrication and properties of high- $T_c$  tapes and coils made from silver-clad Bi-2223 superconductors. IEEE Trans. on Applied Superconductivity 3 (1993) pp. 1127-1130.
- [ 15] Abeln, A., Minor, A., Klemt, E., Reiss, H.: HTSL-Strombegrenzer: Experimentelle Untersuchungen des Auslöseverhaltens von  $(\text{Bi,Pb})_2\text{Sr}_2\text{Ca}_2\text{Cu}_3\text{O}_x$ . VDI Statusseminar "Supraleitung und Tieftemperaturtechnik", Potsdam Sept. 1992.

- [16] McGinnis, W.C., Jacobs, E.W., Rees, C.D., Jones, T.E.: Pulsed current measurement of the resistive transition and critical current in high  $T_c$  superconductors. *Rev. Sci. Instrum.* 61 (1990), pp. 984-987.
- [17] Goldschmidt, D.: Multiple superconducting transition in ceramic YBaCuO. *Phys. Rev. B.* 1988.
- [18] Dersch, H., Blatter, G.: New critical state model for critical currents in ceramic high- $T_c$ -superconductors. *Phys. Rev. B.* 1988 Vol. 38 No. 16, pp. 11391-11404.
- [19] Lindmayer, M.: High temperature superconductors as current limiters - an alternative to contacts and arcs in circuit breakers? 39th IEEE Holm Conference on Electrical Contacts, Pittsburgh 1993.
- [20] Kanbach, H., Bochenek, E., Fischer, R., Voigt, H.: Induktive und induktiv-resistive Strombegrenzer mit Supraleitern. VDE Fachbericht 44 „Kontaktverhalten und Schalten“, Berlin 1993.
- [21] Abeln, A.: BMFT-report 13N5735 (1992), unpublished.
- [22] Lindmayer, M.: Simulation of stationary current - voltage characteristics and of back-commutation in rectangular arc channels. 17th Int. Conf. on Electrical Contacts, Nagoya 1994.
- [23] Eckhardt, H.: Numerische Verfahren in der Energietechnik. Teubner Verlag, Stuttgart 1978.
- [24] Touloukian, Y.S. et. al.: Thermophysical properties of matter; Vol. 2: Thermal conductivity; Vol. 5: Specific heat. IFI/Plenum, New York 1970.
- [25] Orehtsky, J., Reilly, K.M., Suenaga, M., Hikata, T., Ueyama, M., Sato, K.: Ac losses in powder-in-tube  $\text{Bi}_2\text{Ca}_2\text{Cu}_3\text{O}_x$  tapes at power frequencies. *Appl. Phys. Lett.* 60 (1992) pp. 252-254.
- [26] Itoh, T., Miyamoto, T., Wada, Y., Mori, T., Sasao, H.: Design considerations on the Permanent Power Fuse for a motor control center. *IEEE Trans. PAS-92* (1973) pp. 1292-1297.
- [27] Hansson, T., Karlström, P.-O.: Device for motor and short-circuit protection. *Int. Pat. Publication WO 91/12643* (1991).
- [28] Doljack, F.A.: PolySwitch PTC devices - A new low-resistance conductive polymer-based PTC device for overcurrent protection. *IEEE Trans. CHMT-4* (1981) pp. 372-378.
- [29] Perkins, R.S. et al.: A new PTC Resistor for power applications. *IEEE Trans. CHMT-5* (1982) pp. 225-230.
- [30] Hansson, Th.: Polyäthylen-Stromwächter für den Kurzschlußschutz. *ABB Technik* 4/92 pp. 35-38.
- [31] Hansson, Th.: PTC Element. European Patent Application EP 0487 920 A1 (1991).
- [32] Raychem PolySwitch Sicherungselemente. Technical brochure, 1992.
- [33] Bourns MultiFuse overcurrent protection devices. Technical brochure.
- [34] Kleinheins (editor): Elektrisch leitende Kunststoffe. Carl Hanser Verlag, München 1986.
- [35] Hemminger, W.F., Cammenga, H.F.: Methoden der thermischen Analyse. Springer-Verlag, Berlin 1989.

# **COORDINATION WITH ELECTRICAL SYSTEMS**

1. Introduction  
2. The Problem  
3. The Solution  
4. Conclusion

# COORDINATION WITH

# ELECTRICAL SYSTEMS

The first part of the book discusses the basic principles of coordination in electrical systems. It covers the various types of faults that can occur and the methods used to detect and clear them. The second part of the book deals with the coordination of protection devices, such as circuit breakers and fuses, to ensure that they operate in a coordinated manner. This involves the selection of appropriate settings for the protection devices and the coordination of their operating times. The third part of the book discusses the coordination of protection devices in a power system, taking into account the various types of faults and the requirements of the system. The fourth part of the book discusses the coordination of protection devices in a power system, taking into account the various types of faults and the requirements of the system.

The book is written in a clear and concise style, making it easy to read and understand. It is a valuable resource for anyone involved in the design and operation of electrical systems. The book is divided into four main sections: Introduction, The Problem, The Solution, and Conclusion. Each section is further divided into sub-sections, providing a detailed and comprehensive overview of the subject. The book is written in a clear and concise style, making it easy to read and understand. It is a valuable resource for anyone involved in the design and operation of electrical systems.